Published in Applied Optics **43**(3), 585–591 (2004).

Polarized light scattering by dielectric and metallic spheres on oxidized silicon surfaces

Jung Hyeun Kim,[a,b] Sheryl H. Ehrman,[b] George W. Mulholland,[c] and Thomas A. Germer[a]
[a]*Optical Technology Division, National Institute of Standards and Technology, Gaithersburg, MD 20899*
[b]*Department of Chemical Engineering, University of Maryland, College Park, MD 20742*
[c]*Fire Research Division, National Institute of Standards and Technology, Gaithersburg, MD 20899*

Electronic mail: thomas.germer@nist.gov

Abstract: The polarization and intensity of light scattered by polystyrene latex (PSL) and copper spheres with diameters of approximately 100 nm deposited onto silicon substrates containing various thickness of oxide films were measured using 532 nm light. The results are compared with a theory for scattering by a sphere on a surface, originally developed by others [Physica A **137**, 209 (1986)] and extended to include coatings on the substrate. Non-linear least squares fits of the theory to the observations yield results that were consistent with differential mobility measurements of the particle diameter.

OCIS codes: 240.0240, 290.0290, 350.4990, 120.5820

1. Introduction

Various industries use optical scattering to inspect materials for particulate contaminants, roughness, and other defects.[1] Inspection tools that can distinguish amongst different types of defects can improve yield management by identifying sources of defects. The development of optimized inspection tools is thus aided by the availability of accurate models for light scattering. With this goal in mind, a number of theories have been developed to predict the scattering by particles on surfaces.[2-12] Validation of those theories, however, has been carried out only in a limited number of cases, and measurements have been performed primarily using dielectric spheres on bare substrates.[9,13-17] Few studies have described measurements using metallic particles, or particles on dielectric films. Metallic particles mimic those found in many manufacturing environments and provide significant challenges to the available theories. Dielectric films are often present on surfaces, and the presence of such films can significantly alter the scattering properties of the particles.

The use of optical scattering to accurately size reference particles on surfaces is growing.[18,19] While approximate theories for scattering can be used to guide the development of inspection tools, it is essential that accurate theories be available when those theories are being used as the basis for sizing reference particles. The basis of a complete evaluation of the uncertainties in those measurements requires that all non-ideal conditions be assessed and evaluated for their effect on the scattering behavior. The ability to accurately size reference particles can only be as good as the theories used to interpret the scatter.

In this article, we describe measurements of the scattering of light by polystyrene latex (PSL) and copper spheres deposited onto oxidized silicon wafers. We use the measurements to validate an extension of the theory of Bobbert and Vlieger,[2] which includes the presence of the substrate film. While

approximate models are often used to predict scattering by particles, we point out a few pitfalls that are encountered with two common approximations. We then perform a non-linear least-squares fit of the model to the data to determine the diameters of the particles on each substrate. The results show excellent agreement with each other and with other measurements of the particle size. Since the scattering by copper particles is strongly dependent upon shape, and the substrate oxide thickness when it is very thin, these results suggest that optical scattering measurements of particle size can be most accurately performed when an intentionally grown oxide exists on the substrate.

2. Theory

Bobbert and Vlieger (BV) developed a theory for light scattering by a spherical particle above a planar surface.[2] Using spherical harmonics as a basis for an expansion of the Debye potentials, BV derived the surface reflection matrix **A**. Thus, they could self-consistently include the presence of the surface into the Mie scattering solution for a sphere. The only approximation was that the scattered field was to be evaluated at a large distance from the particle. While the original BV theory did not include the existence of layers on either the substrate or the particle, the expressions for the matrix **A** were written with respect to the Fresnel reflection coefficients of the surface and the Mie scattering coefficients of the sphere, and the extension of the theory to include the existence of any layers is straightforward. The complete implementation details of the BV theory were described in a previous paper,[17] and the code has been included in a library of scattering models available on the Internet.[20]

Two approximations have been commonly reported in the past. The Mie-Surface Double Interaction (MSDI) model, developed by Nahm and Wolfe,[3] ignores the interaction of the sphere with its image in the substrate. That is, light scattered by the sphere does not contribute to the light incident upon the sphere. In the absence of any films, the model is valid when the particle is small, and either the substrate or the particle has an index close to one. The model can be evaluated using our implementation by ignoring the interaction of the sphere with its image in the substrate, that is, by setting the near-field reflection matrix **A** to zero. Use of the Normal Incidence Approximation (NIA), developed by Videen,[4,5] requires the assumption that, for the calculation of the reflection matrix **A**, the reflection coefficients are independent of angle and are given by their values at normal-incidence: $r(\theta) = r(0)$. The NIA model is valid when the substrate reflection coefficients are not a strong function of angle of incidence. Since this article concerns the scattering by particles above dielectric films, there are regimes where neither the MSDI nor NIA models apply.

Evaluation of the BV theory requires choosing a maximum spherical harmonic order l_m. For PSL spheres, convergence is always rapid, converging to 1 % of the solution when $l_m = 3$. For copper spheres directly touching a silicon surface without any oxide, convergence is extremely slow, failing to converge to an acceptable solution for $l_m = 60$. Fortunately, the convergence rate is significantly improved in the presence of a silicon dioxide layer. For a 1 nm oxide coating, convergence to 1 % of the solution is obtained for copper spheres by $l_m = 20$.

3. Sample Preparation

Silicon wafer substrates were prepared by RCA cleaning[21], followed by dry thermal oxidation[22] for films less than 100 nm or by wet thermal oxidation[23] for micrometer thick films. The resulting film thicknesses were measured using spectroscopic ellipsometry and are summarized in Table 1.

Polystyrene latex (PSL) and copper spheres were deposited onto the substrates using an electrostatic precipitator (ESP) with an electric field (5000 V/cm) between the aerosol stream inlet and the wafer. The PSL spheres consisted of the NIST Standard Reference Material (SRM® 1963)[24] and have a

mean diameter[25] of 100.7 nm ± 1.0 nm and an estimated standard deviation of about 2.2 nm. The copper spheres were produced by spray pyrolysis from copper nitrate and, after electrostatic classification, had a mean diameter[25] of 100.0 nm ± 2.0 nm and an estimated standard deviation of about 2.5 nm. Details of the methodology for obtaining PSL and Cu samples for these measurements were described in previous articles.[17,26] The differential mobility analyzer[27] (DMA) used for the Cu particle classification was calibrated by the PSL spheres. The slight difference between the sizes of the PSL and Cu spheres was a result of that calibration being performed after the deposition. A dark field optical microscope was used to determine the particle number density of deposited copper particles, but it was difficult to measure the number density of the PSL spheres because of their low scattering intensity. The particle number densities of copper spheres were between 250 mm^{-2} and 500 mm^{-2}. The PSL number densities obtained from fits to the data were approximately 4000 mm^{-2}. The complex indices of refraction of PSL, copper, silicon, and silicon dioxide for the model calculations were assumed to be[28,29] 1.598, 1.06 + 2.59*i*, 4.15 + 0.05*i*, and 1.461, at wavelength λ = 532 nm.

4. Optical Scattering Measurements

The goniometric optical scatter instrument, which was used to perform the light scattering measurements, is described in detail elsewhere.[30] Linear polarized light of wavelength λ = 532 nm from a doubled Nd:YAG laser was incident onto each sample at an angle θ_i from the surface normal. The scattered light was analyzed as a function of polar angle θ_r and azimuthal angle ϕ_r for its intensity and polarization state by a rotating $\lambda/4$ retarder followed by a fixed polarizer. Measurements were performed for samples with deposited particles, and otherwise identical witness samples having identical films but no particles. The scattered Stokes vector intensity from the particles was assumed to be

$$\mathbf{\Phi}_r = \mathbf{\Phi}_{r,\text{particle}} - \mathbf{\Phi}_{r,\text{witness}} \tag{1}$$

where $\mathbf{\Phi}_{r,\text{particle}}$ was the Stokes vector intensity measured from the particle-covered sample, and $\mathbf{\Phi}_{r,\text{witness}}$ was the Stokes vector intensity measured from the witness sample. The differential scattering cross section is given by

$$\frac{\mathrm{d}\sigma}{\mathrm{d}\Omega} \cong \frac{\Phi_{r,0}\cos\theta_i}{\Phi_i\,\rho\,\Omega} \tag{2}$$

where $\Phi_{r,0}$ is the first (intensity) element of the Stokes vector $\mathbf{\Phi}_r$, Φ_i is the measured incident power, Ω is solid angle of collection, and ρ is the surface number density of particles. The incident light was polarized 45° from the plane of incidence to yield high polarimetric differentiation among different samples. Measurements are presented in the plane of incidence for a fixed incident angle θ_i = 60°, scanning the viewing angle θ_r. The polarization state of the light is parameterized by its principal angle of polarization η, its degree of circular polarization P_C, and its total degree of polarization P. With respect to the Stokes parameters, these parameters are given by:

$$\eta = \frac{1}{2}\arctan(\Phi_{r,1}, \Phi_{r,2}) \tag{3a}$$

$$P_C = \Phi_{r,3} / \Phi_{r,0} \tag{3b}$$

$$P = \left(\Phi_{r,1}{}^2 + \Phi_{r,2}{}^2 + \Phi_{r,3}{}^2 \right)^{1/2} / \Phi_{r,0} \qquad (3c)$$

The angle η is measured from s-polarization in a right-handed fashion (counterclockwise, looking into the beam). The value of P_C is positive for left-circularly polarized light. We show the normalized degree of circular polarization P_C/P because some depolarization was observed. The normalized value is more appropriate to compare to theory, since all of the theories predict $P = 1$. While a complete uncertainty analysis has not been performed for these measurements, the uncertainties in $d\sigma/d\Omega$, η, P_C, and P are expected to be dominated by statistical sources and can be estimated by the point to point fluctuations in the observed data.

While we have subtracted the signal of a witness wafer from the experimental data, we do not show results in directions where the witness wafer signal is close to or greater than that of the particle signal. For example, near the specular direction at $\theta_r = 60°$, scatter is dominated by surface roughness and flatness rather than the particles. Experimental data are also not shown for large scattering angles, $|\theta_r| > 60°$, because the scattering was found to be dominated by background sources. In all measured data, we observed some depolarization, which may be the combined result of incomplete subtraction of the background signal, the finite width of the particle size distribution, non-sphericity of the particles, multiple scattering from particles, or from foreign particles.

5. Results and Discussion

The approximations used in a number of other studies have shortcomings when applied to the scattering of particles above substrates with coatings. For example, the NIA model assumes that the reflection coefficients of the surface are independent of angle and equal to those evaluated at normal incidence. For coated surfaces, the reflection coefficients can be a strong function of angle. For metallic particles, which can exhibit strong near field scattered fields, the reflection coefficients observed by the particle extend far beyond those evaluated at normal incidence. Figure 1 shows comparisons of the MSDI model, NIA model, and the BV theory for a 100 nm copper sphere on a silicon wafer having a 160 nm SiO_2 film. The particular film thickness used in Fig. 1 was chosen because it illustrates an extreme condition. The normal incidence reflectance of the substrate is close to that of the bare substrate. The BV theory and the NIA model differ significantly. In fact, the MSDI model, which completely ignores the interaction of the sphere with the substrate altogether, agrees much better with the BV theory. For very thin oxides, the MSDI model tends to fail, while for thicker oxides, the NIA model tends to fail. In the remainder of this article, the complete BV theory will be used.

One purpose of this study was to test the validity of the extension to the BV theory for scattering by spherical particles on substrates with dielectric films. Figures 2 and 3 show light scattering parameters measured in the plane of incidence using 45°-polarized light of wavelength $\lambda = 532$ nm for the PSL and copper spheres, respectively, each on three films less than 100 nm thick. The absolute $d\sigma/d\Omega$ for the data was adjusted by a constant factor for each data set, which accounts for the uncertainty in the particle number density. Both particles produced excellent agreement with the BV theory for the polarization and differential scattering cross section.

Interestingly, the results of the scattering parameters show similar trends as those observed when the particle size is varied. Figure 4 shows a demonstration of the correlation between particle size and substrate film thickness. The calculated scattering by a 100 nm copper sphere above an 18 nm oxide was non-linear least squares fitted to the theory for an unknown diameter copper sphere above a 1.5 nm oxide, letting the unknown copper sphere diameter and an overall scaling of the cross section be free parameters. The resulting best fit yielded a diameter of 119 nm (and a relative scale factor of about 0.6), showing an

approximately 1:1 sensitivity of oxide thickness to sphere diameter. While the fit shown in Fig. 4 is not perfect, the similarity between the curves demonstrates the importance of independently determining the oxide thickness in particle size measurements.

In addition to measurements with thin oxides, we also performed measurements with thicker oxides. Figures 5 and 6 show the results of light scattering by PSL and Cu spheres on 2077 nm and 2086 nm films, respectively. The overall agreement of the data with the BV predictions is excellent. The results show significantly more structure than those on thin films, due to constructive and destructive interference in the thick film.

In order to assess the use of the scatter measurements to determine particle size, we performed non-linear least square fits of the data to the BV theory. For these calculations, a weighted Levenberg-Marquardt algorithm was used, letting the density and particle diameter be free parameters. The weights were determined by estimating the uncertainty in each data point, and curvatures of the estimated chi-squared were used to determine uncertainties in the fits. These methods are outlined in Ref. 31. These uncertainty estimates, however, do not represent a complete estimate of the systematic measurement errors, but only those which result from the statistical errors. In a previous study, it was demonstrated that significant systematic errors can result from uncertainties in the optical properties of the substrate and film, the thickness of the film, uncertainty in the shape of the particles, presence of doublet particles, and polydispersity of the particle size distribution.[19] In these measurements, the incident angle, polarization, and wavelength were not optimized to obtain the most accurate measurement of particles of this size.

Fits were performed on each parameter ($d\sigma/d\Omega$, P_C, and η) separately and on all of them as a whole. Table 2 shows a summary of the results of these fits. Nearly all of the fits yield values in reasonable agreement with the size determined by differential mobility analysis, when the uncertainties are taken into consideration. Some of the fits yielded large estimated uncertainties, such as most of those for P_C, and the uncertainties were reduced substantially by including all of the scattering parameters in the fits. Furthermore, there were no significant trends in the uncertainty or the best-fit diameter as film thickness was varied, except to note that values farthest from the mean were generally from the samples with only a native oxide. Fits to single parameters sometimes yielded large uncertainties when the film thickness was such that that parameter was relatively insensitive to diameter. The weighted average and weighted uncertainty[25] of the diameter when all of the parameters were fit was 102.0 nm ± 1.4 nm for the PSL spheres and 99.9 nm ± 1.2 nm for the Cu spheres. The quality of the fits and their overall agreement with the size determined by differential mobility analysis supports the accuracy of the model calculations.

6. Conclusion

Polarized light scattering by PSL and copper spheres on oxidized silicon surfaces was measured and the results were compared to the predictions of the theory of Bobbert and Vlieger. We show that the scattering depends upon the film thickness. For accurate particle sizing, the film thickness must be independently determined, since there is a strong correlation between film thickness and estimated particle size. Results of non-linear least squares fitting show improved uncertainties can be obtained by fitting the entire differential cross section and polarization state simultaneously.

References

1. J. C. Stover, *Optical Scattering: Measurement and Analysis*, (SPIE Optical Engineering Press, Bellingham, WA, 1995).
2. P. A. Bobbert and J. Vlieger, "Light scattering by a sphere on a substrate," Physica **137A**, 209-242 (1986).
3. K. B. Nahm and W. L. Wolfe, "Light-scattering models for spheres on a conducting plane: comparison with experiment," Appl. Opt. **26**, 2995-2999 (1987).
4. G. Videen, "Light scattering from a sphere on or near a surface," J. Opt. Soc. Am. A **8**, 483-489 (1991).

5. G. Videen, "Light scattering from a sphere on or near a surface: errata," J. Opt. Soc. Am. A **9**, 844-845 (1992).
6. G. Videen, M. G. Turner, V. J. Iafelice, W. S. Bickel, and W. L. Wolfe, "Scattering from a small sphere near a surface," J. Opt. Soc. Am. A **10**, 118-126 (1993).
7. Yu. Eremin and N. Orlov, "Simulation of light scattering from a particle upon a wafer surface," Appl. Opt. **35**, 6599--6604 (1996).
8. E. Fucile, P. Denti, F. Borghese, R. Saija, and O. I. Sindoni, "Optical properties of a sphere in the vicinity of a plane surface," J. Opt. Soc. Am. A **14**, 1505-1514 (1997).
9. R. Schmehl, B. M. Nebeker, and E. D. Hirleman, "Discrete-dipole approximation for scattering by features on surfaces by means of a two-dimensional fast Fourier transform technique," J. Opt. Soc. Am. A **14**, 3026-3036 (1997).
10. Yu. Eremin and N. Orlov, "Modeling of light scattering by non-spherical particles based on discrete sources method," J. Quant. Spectrosc. Radiat. Transfer. **60**, 451-462 (1998).
11. Y. A. Eremin, J. C. Stover, and N. V. Orlov, "Modeling scatter from silicon wafer features based on discrete sources method," Opt. Eng. **38**, 1296-1304 (1999).
12. A. Doicu, Yu. Eremin, and T. Wriedt, "Non-axisymmetric models for light scattering from a particle on or near a plane surface," Opt. Commun. **182**, 281-288 (2000).
13. D. C. Weber and E. D. Hirleman, "Light scattering signatures of individual spheres on optically smooth conducting surfaces," Appl. Opt. **27**, 4019-4026 (1988).
14. L. Sung, G. W. Mulholland, and T. A. Germer, "Polarized light-scattering measurements of dielectric spheres upon a silicon surface," Opt. Lett. **24**, 866-868 (1999).
15. B. Kaplan and B. Drevillon, "Mueller matrix of dense polystyrene latex sphere suspensions: measurements and Monte Carlo simulation," Appl. Opt. **40**, 2769-2777 (2001).
16. B. Kaplan and B. Drevillon, "Mueller matrix measurements of small spherical particles deposited on a c-Si wafer," Appl. Opt. **41**, 5405-5412 (2002).
17. J. H. Kim, S. H. Ehrman, G. W. Mulholland, and T. A. Germer, "Polarized light scattering by dielectric and metallic spheres on silicon wafers," Appl. Opt. **41**, 5405-5412 (2002).
18. J.C.Stover and C.A.Scheer, "Accurate sizing of deposited PSL spheres from light scatter measurements," in *Optical Metrology Roadmap for the Semiconductor, Optical, and Data Storage Industries II*, A.Duparré and B.Singh, Eds., Proc. SPIE **4449**, 147–150 (2001)
19. T.A.Germer, G.W.Mulholland, J.H.Kim, and S.H.Ehrman, "Measurement of the 100 nm NIST SRM® 1963 by laser surface light scattering," in *Advanced Characterization Techniques for Optical, Semiconductor, and Data Storage Components*, A.Duparré and B.Singh, Eds., Proc. SPIE **4779**, 60–71 (2002)
20. T.A.Germer, *SCATMECH: Polarized Light Scattering C++ Class Library*, available at http://physics.nist.gov/scatmech (2000).
21. W. Kern and D. A. Puotinen, "Cleaning solutions based on hydrogen peroxide for use in silicon semiconductor technology," RCA Review **30**, 187-206 (1984).
22. C. R. Helms and C.-J. Han, "Parallel oxidation mechanism for Si oxidation in dry O_2," *J.* Electrochem. Soc. **134**, 1297-1302 (1987).
23. Y. Wang, J. Tao, S. Tong, T. Sun, A. Zhang, and S. Feng, "The oxidation kinetics of thin polycrystalline silicon films," J. Electrochem. Soc. **138**, 214-219 (1991).
24. G. W. Mulholland, N. P. Bryner, and C. Croarkin, "Measurement of the 100 nm NIST SRM 1963 by differential mobility analysis," Aerosol Sci. and Technol. **31**, 39-55 (1999).
25. Unless otherwise noted, the uncertainties quoted in this article were obtained by estimating the standard uncertainty *u* for the measurement and multiplying by a coverage factor of $k = 2$. These values correspond to a confidence level of 95 %.
26. J. H. Kim, T. A. Germer, G. W. Mulholland, and S. H. Ehrman, "Size-monodisperse metal nanoparticles via hydrogen-free spray pyrolysis," Adv. Mater. **14**, 518-521 (2002).
27. P. D. Kinney, D. Y. H. Pui, G. W. Mulholland, and N. P. Bryner, "Use of the electrostatic classification method to size 0.1 µm SRM particles—a feasibility study," J. Res. Natl. Inst. Stand. Technol. **96**, 147 (1991).
28. E. D. Palik, *Handbook of Optical Constants of Solids*, (Academic, San Diego, 1985).
29. *Styrene, Its Polymers, Copolymers, and Derivatives*, R. H. Boundy and R. F. Boyer, eds., (Reinhold, New York, 1952).
30. T. A. Germer and C. C. Asmail, "Goniometric optical scatter instrument for out-of-plane ellipsometry measurements," Rev. Sci. Instr. **70**, 3688-3695 (1999).
31. W. H. Press, S. A. Teukolsky, W. T. Vetterling, and B. P. Flannery, *Numerical Recipes in C: The Art of Scientific Computing*, (Cambridge, Cambridge University, 1992).

Table 1. Oxide growth conditions and resulting film thicknesses

Growth condition	Film Thickness (nm)[a]	
	For PSL	For Cu
900 ^{o}C for 23 min (Dry O_2)	18 ± 2	18 ± 2
1000 ^{o}C for 18 min (Dry O_2)	45 ± 1	40 ± 1
1000 ^{o}C for 60 min (Dry O_2)	66 ± 1	65 ± 1
1100 ^{o}C for 6000 min (Wet O_2)	2077 ± 1	2086 ± 1

Dry O_2: Oxygen flow rate = 7 L min^{-1}
Wet O_2: Oxygen flow rate = 0.15 L min^{-1}, and hydrogen flow rate = 0.10 L min^{-1}
[a] See Note 25.

Table 2. Results of non-linear least square fits of the BV theory to the data. The uncertainties represent an estimate of the standard uncertainty of the fitting parameters.

PSL 100.7 nm			Cu 100.0 nm		
Film Thickness (nm)	Fitting Parameter	Estimated Diameter (nm)	Film Thickness (nm)	Fitting Parameter	Estimated Diameter (nm)
Native Oxide (1.5)	dσ/dΩ	105.5 ± 1.8	Native Oxide (1.5)	dσ/dΩ	102.2 ± 0.6
	P_c	109.8 ± 11.4		P_c	106.8 ± 3.1
	η	102.4 ± 17.8		η	102.4 ± 8.3
	All	102.6 ± 0.8		All	102.5 ± 0.3
18	dσ/dΩ	103.5 ± 1.9	18	dσ/dΩ	97.7 ± 1.5
	P_c	106.2 ± 10.7		P_c	100.6 ± 11.4
	η	103.2 ± 6.6		η	98.8 ± 6.6
	All	102.3 ± 0.4		All	99.0 ± 0.4
45	dσ/dΩ	101.1 ± 15.5	40	dσ/dΩ	99.7 ± 7.4
	P_c	101.1 ± 16.5		P_c	111.9 ± 18.6
	η	98.4 ± 15.3		η	109.9 ± 18.0
	All	99.1 ± 1.0		All	100.0 ± 1.4
66	dσ/dΩ	98.2 ± 9.7	65	dσ/dΩ	98.7 ± 17.8
	P_c	115.7 ± 22.3		P_c	102.1 ± 27.8
	η	115.8 ± 25.0		η	97.4 ± 24.5
	All	100.0 ± 3.5		All	99.4 ± 2.7
2077	dσ/dΩ	100.9 ± 2.8	2086	dσ/dΩ	101.1 ± 2.4
	P_c	102.1 ± 30.3		P_c	104.0 ± 21.3
	η	100.7 ± 51.8		η	99.6 ± 6.4
	All	101.0 ± 2.6		All	99.8 ± 0.4

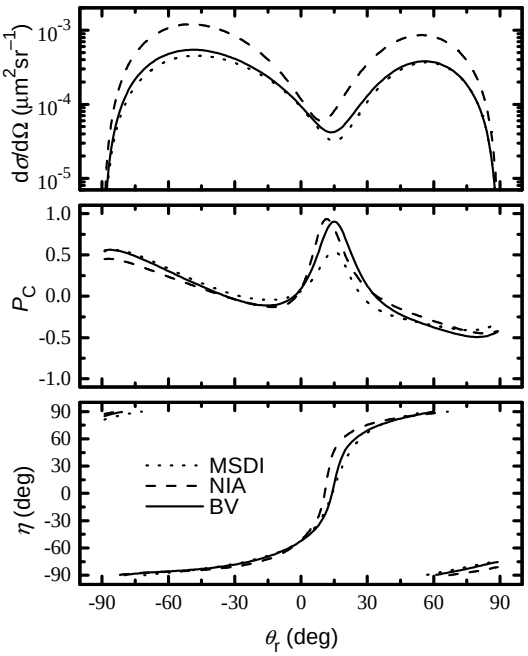

Fig. 1. Light scattering parameters for a 100 nm copper sphere on a silicon substrate having 160 nm SiO_2 film predicted by the MSDI model, NIA model, and the BV theory in the plane of incidence with $\theta_i = 60°$ and $\lambda = 532$ nm.

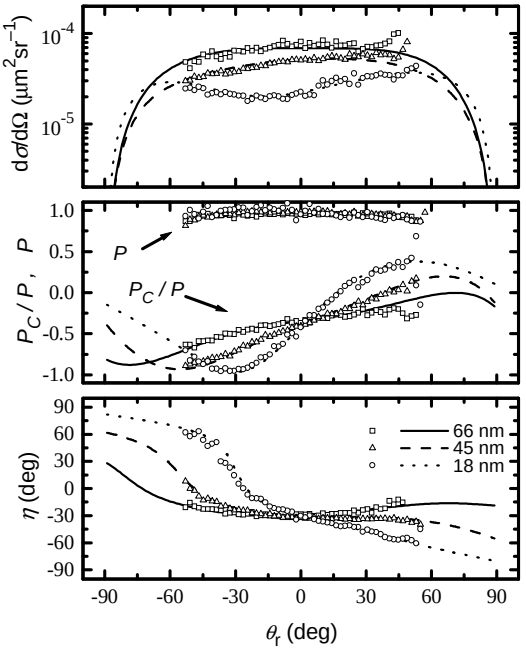

Fig. 2. Light scattering parameters for a 101 nm PSL sphere on a silicon substrate with 18 nm, 45 nm, and 66 nm SiO_2 films measured in the plane of incidence with $\theta_i = 60°$ and $\lambda = 532$ nm. The curves represent the predictions of the BV theory.

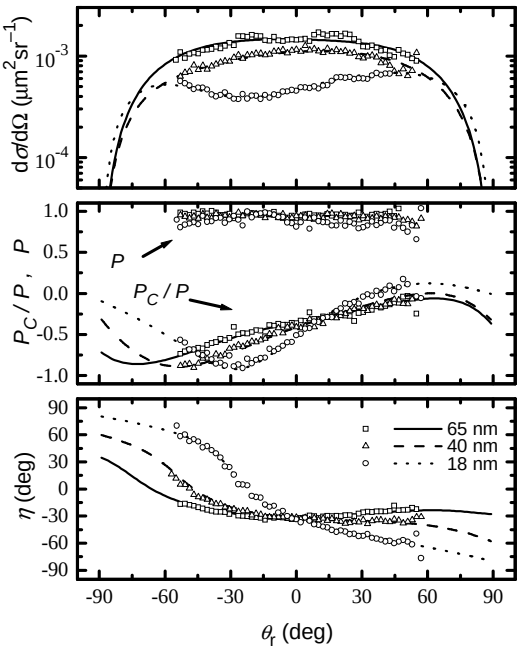

Fig. 3. Light scattering parameters for a 100 nm copper sphere on a silicon substrate with 18 nm, 40 nm, and 65 nm SiO_2 films measured in the plane of incidence with $\theta_i = 60°$ and $\lambda = 532$ nm. The curves represent the predictions of the BV theory.

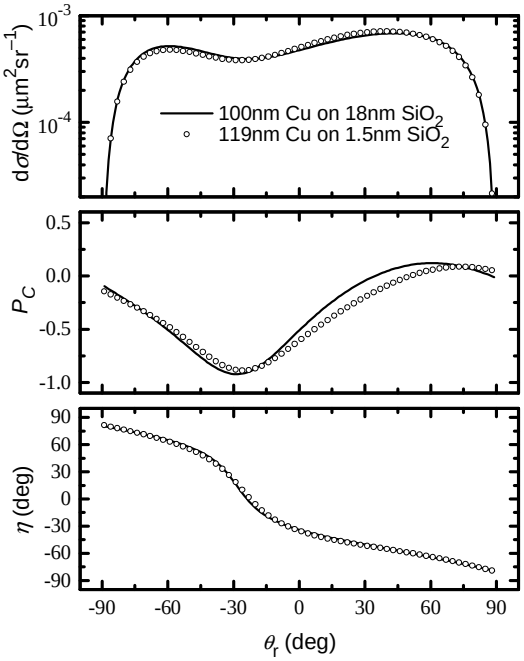

Fig. 4. Light scattering parameters for a 100 nm copper sphere on a silicon substrate with 18 nm SiO_2 film calculated in the plane of incidence with $\theta_i = 60°$ and $\lambda = 532$ nm. Comparison of the scattering parameters is made with the scattering by a 119 nm copper sphere on a silicon substrate with 1.5 nm native oxide. The cross section for the 119 nm copper spheres has been multiplied by a factor of 0.6.

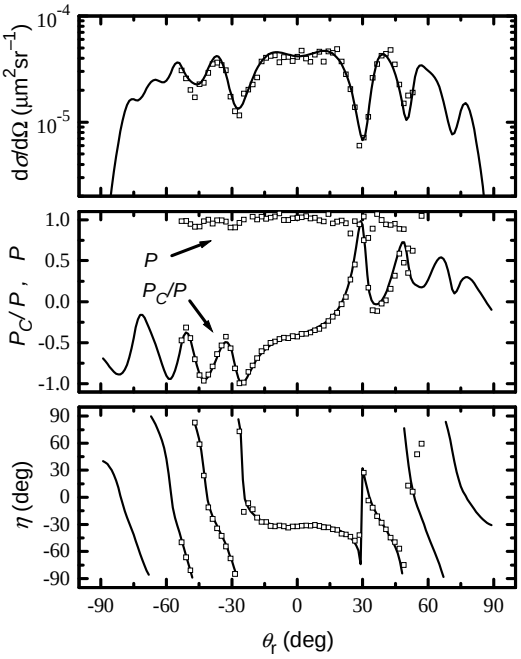

Fig. 5. Light scattering parameters for a 101 nm PSL sphere on a silicon substrate with 2077 nm SiO_2 films measured in the plane of incidence with $\theta_i = 60°$ and $\lambda = 532$ nm. The curves represent the predictions of the BV theory.

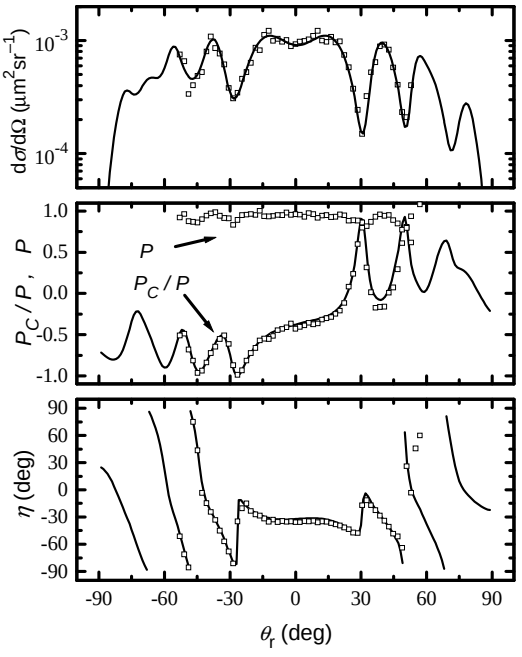

Fig. 6. Light scattering parameters for a 100 nm copper sphere on a silicon substrate with 2086 nm SiO_2 films measured in the plane of incidence with $\theta_i = 60°$ and $\lambda = 532$ nm. The curves represent the predictions of the BV theory.